

Evolution and the concomitant disappearance of high- T_c superconductivity with carrier concentration in the $\text{La}_{2-x}\text{Sr}_x\text{CuO}_{4-\delta}$ system ($0.0 < x < 1.2$): Crossover from a Mott insulator to a band metal

K. Sreedhar and P. Ganguly

Solid State and Structural Chemistry Unit, Indian Institute of Science, Bangalore 560 012, India

(Received 9 May 1989)

Electrical resistivity, magnetic susceptibility, thermogravimetric analysis, and infrared absorption spectra of the compound $\text{La}_{2-x}\text{Sr}_x\text{CuO}_{4-\delta}$ have been studied for a wide range of Sr concentrations ($0.0 \leq x \leq 1.2$). The samples annealed at an oxygen pressure of 1 bar were stoichiometric ($\delta=0.0$) in the range $0.0 < x < 0.33$. In this range the compounds are characterized by a decrease in the a parameter, an increase in the c parameter, and a maximum in the c/a ratio (at $x=0.33$) typical of the formation of low-spin Cu^{3+} ions. In the range $0.15 < x < 0.33$, the compounds show a positive temperature coefficient of resistivity, decrease in the magnitude of the Pauli magnetic susceptibility, infrared oscillator strengths, thermopower S , as well as the Hall coefficient R_H . The superconducting transition temperature T_c as well as the percentage Meissner fraction also decrease with x in this range. In particular the stoichiometric $x=0.33$ composition having a hole concentration of ~ 0.33 holes/Cu shows a minimum in the Pauli magnetic susceptibility and disappearance of all infrared absorption bands. The superconductivity also disappears down to 4.2 K at this composition, even though it is more metallic. These results have been attributed to the occurrence of a transition from a highly correlated narrow-band "Mott conductor" to a broadband metal at high carrier concentrations. At still higher Sr concentrations ($0.33 < x < 1.0$), holes and oxygen vacancies coexist. The decrease in the c/a ratio, increase in resistivity, reappearance of the infrared bands, and the Curie-type magnetic susceptibility observed in the range $0.66 \leq x \leq 1.2$ indicate the dominating role of oxygen vacancies which induce disorder and localization.

I. INTRODUCTION

Since the discovery of high-temperature superconductivity¹ ($T_c > 30$ K) in the La-Ba (Sr)-Cu-O system with K_2NiF_4 -type structure, several mixed valent metallic copper oxides are known to show high-temperature superconductivity.²⁻⁵ Most of these compounds have low-dimensional structural features and show high anisotropy in the electrical transport properties. The superconducting transition temperature T_c depends on the oxygen stoichiometry, carrier concentration, as well as dimensionality in these systems. The absence of high- T_c superconductivity in some of the mixed valent metallic copper oxides,⁶ for instance $\text{La}_4\text{BaCu}_5\text{O}_{13}$, seems to be associated with the absence of low-dimensional structural features⁷ in these compounds. Since the $\text{La}_{2-x}\text{Sr}_x\text{CuO}_{4-\delta}$ system is known to be stable in the K_2NiF_4 -type structure⁸ (Fig. 1) for a wide composition range ($0.0 < x < 1.33$), this system is ideally suited to study the effect of oxygen stoichiometry and carrier concentration, on the magnetic and electrical transport properties, particularly the superconducting transition temperature T_c .

Even though a large number of studies have been carried out in this system for the last two years, most of the studies have concentrated only in the limited range of Sr concentration where the high- T_c superconductivity is observed. In particular, these studies have shown that in

the range $0.05 < x < 0.15$ the T_c increases from ~ 10 to 38 K and further increase in x decreases the T_c in this system.⁹ The observed decrease in T_c when $x > 0.15$ has earlier been attributed to the formation of oxygen vacancies. In fact, the earlier structural and thermogravimetric analysis (TGA) studies^{8,10} have shown unambiguously that the system is stoichiometric up to $x \sim 0.33$ when the compounds are annealed at an oxygen pressure of 1 bar. Recently Torrance *et al.*⁹ have been able to increase the stoichiometric range in this system up to $x=0.40$ by treating the compounds at an oxygen pressure of 100 bar. Moreover, on the basis of percentage Meissner effect, they have shown that in the metallic stoichiometric samples ($0.30 < x < 0.40$) having a high-hole concentration, the superconductivity "anomalously" disappears down to 5 K.

In this paper we report our investigations on the $\text{La}_{2-x}\text{Sr}_x\text{CuO}_{4-\delta}$ system in the normal state for a wide range of Sr concentration ($0 \leq x \leq 1.2$). In particular, we have studied the "anomalous" disappearance of high- T_c superconductivity at high-hole concentrations using thermogravimetric analysis, electron diffraction, infrared absorption spectra, magnetic susceptibility, and electrical resistivity. The results are correlated with their structure, oxygen stoichiometry, and carrier concentration which, in turn, determines the superconducting transition temperature in these systems.

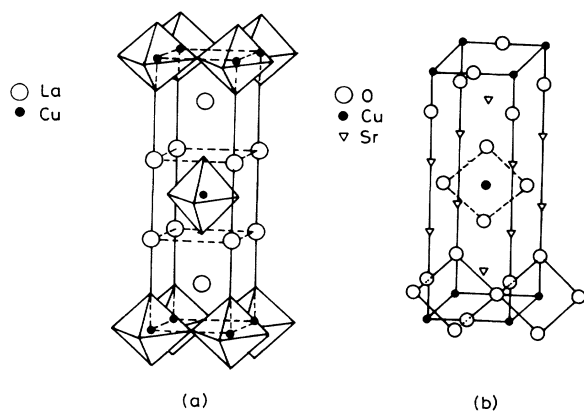


FIG. 1. Relationship between the crystal structure of La_2CuO_4 (a) (drawn as ideal K_2NiF_4 -type structure with octahedral coordination for Cu^{2+} ions) to that of Sr_2CuO_3 , (b) with square-planar coordination for the Cu^{2+} ions (from Ref. 15).

II. EXPERIMENT

$\text{La}_{2-x}\text{Sr}_x\text{CuO}_4$ ($0 \leq x \leq 1.2$) compounds were prepared in air by grinding appropriate amount of La_2O_3 , SrCO_3 , and CuO (>99.9% purity) under acetone, and heating in a platinum boat for 12 h first at 1200 K and then at temperatures ranging from 1300 to 1475 K for 48 h, with intermittent grinding and pelletizing. For the compositions having high Sr concentrations ($0.33 < x < 1.2$), heating above 1400 K is essential for obtaining a well crystalline single phase.⁸ These compounds are then annealed at 700 K for 12 h under an oxygen pressure of 1 bar. The x-ray diffraction patterns of the compounds showed that all are single-phase materials with tetragonal K_2NiF_4 -type structure. The oxygen stoichiometry was determined by thermogravimetric reduction in hydrogen using a Sartorius microbalance as well as chemically by iodometric titration. In the former method it is assumed that only the copper would undergo reduction to the metallic state so that from the weight loss one could calculate the oxygen stoichiometry. Both the methods gave nearly identical results. The TGA results are fairly independent of particle size (<40 microns), flow rate of hydrogen (5–20 ml per minute) and the heating rate (1–5 K per minute) employed.

X-ray diffraction patterns were recorded with a JEOL-8p diffractometer using $\text{Cu } K\alpha$ radiation. Magnetic susceptibility was measured by the Faraday method using a Cahn-RG electrobalance down to 14 K. Electrical resistivity was measured by the standard four-probe method. Infrared spectra were recorded using a Perkin Elmer spectrometer. Electron diffraction pattern and the lattice image were obtained using a JEOL 200 CX electron microscope.

III. RESULTS AND DISCUSSION

A. Oxygen stoichiometry

In Fig. 2 we compare the TGA results of the $\text{La}_{2-x}\text{Sr}_x\text{CuO}_{4-\delta}$ system in hydrogen, with some model

compounds Y_2BaCuO_5 , BaO_2 , and $\text{La}_4\text{LiCuO}_8$ containing isolated Cu^{2+} ,¹¹ peroxide¹² and Cu^{3+} ions,¹³ respectively. From this figure it is seen that the compounds containing Cu^{3+} or O_2^{2-} ions get reduced at a lower temperature than those having Cu^{2+} ions, as expected from the redox potentials.¹⁴ It also shows that the reduction takes place in one step in the case of BaO_2 and Y_2BaCuO_5 . A slight initial increase in the weight on reduction of BaO_2 suggests a dissociative adsorption of hydrogen with the formation of $\text{Ba}(\text{OH})_2$ and a subsequent dehydration.

TGA data of the $\text{La}_{2-x}\text{Sr}_x\text{CuO}_{4-\delta}$ [Fig. 2(b)] show that for the parent $x=0.0$ compound, the reduction takes place in one step, like that of Y_2BaCuO_5 . But for $x > 0.0$ samples, the reduction is in two steps, indicating different local effects associated with La^{3+} and Sr^{2+} ions on the reduction process. In contrast to the $x < 0.33$ samples the oxygen-deficient $x > 0.5$ samples show a propensity to absorb moisture and get hydrolyzed like Sr_2CuO_3 ,¹⁵ when kept exposed in the ambient laboratory atmosphere for a long time.

The TGA data also show that the compound $\text{La}_{2-x}\text{Sr}_x\text{CuO}_{4-\delta}$ is stoichiometric ($\delta=0.0$) in the range

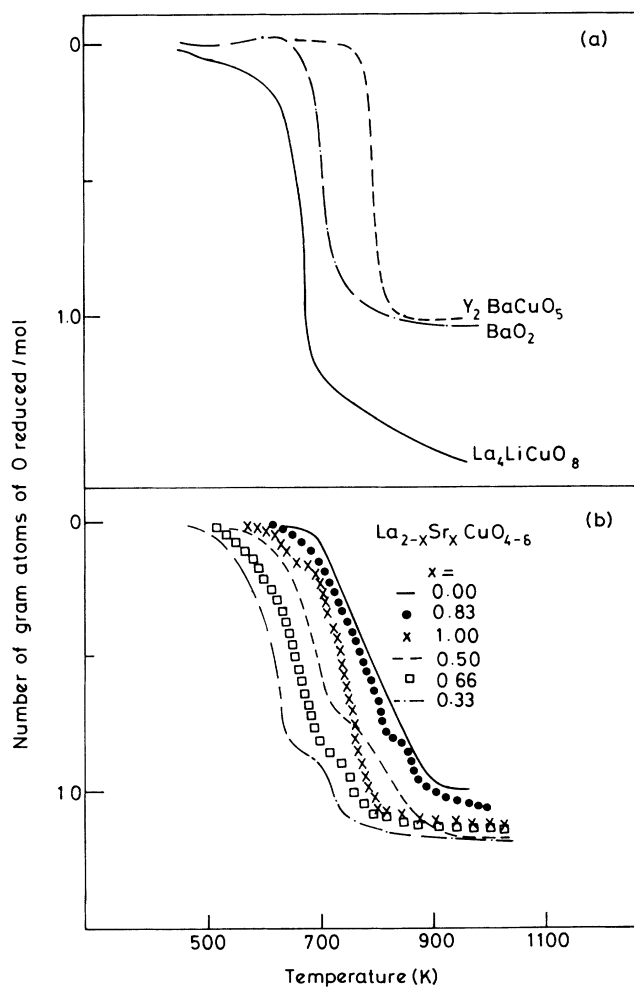


FIG. 2. TGA data of Y_2BaCuO_5 , BaO_2 , and $\text{La}_4\text{LiCuO}_8$ (a) and some members of the $\text{La}_{2-x}\text{Sr}_x\text{CuO}_{4-\delta}$ ($0.0 < x < 1.2$) series (b) reduced in the hydrogen atmosphere.

($0.0 < x < 0.33$), and the number of holes increase linearly with x , when the samples are annealed at an oxygen pressure of 1 bar (Fig. 3). At higher Sr concentrations ($0.33 < x < 1.0$) the percentage of holes remain almost constant ($\sim 30\%$). This has also been confirmed by the chemical analysis, employing iodometric titration. This saturation of hole concentration at higher values of x ($0.33 < x < 1.2$) is due to the creation of oxygen vacancies as evidenced by the electron diffraction.⁸ For example, the electron diffraction pattern of the $\text{La}_{0.8}\text{Sr}_{1.2}\text{CuO}_{4-\delta}$ samples along the (001) direction [Fig. 4(a)] shows superstructure [$(5 \times)$ a K_2NiF_4] reflections due to ordering of oxygen vacancies in the a - b plane. Further evidence for the ordering of oxygen vacancies is seen in the lattice image [Fig. 4(b)] obtained along the [001] direction for this compound. The image shows fringes of $\sim 18 \text{ \AA}$ width corresponding to [$(5 \times)$ a K_2NiF_4].

We have been fairly successful in simulating the oxygen loss from the samples in the range $0.0 < x < 1.0$, by putting the constraints that (a) the Sr^{2+} and La^{3+} ions are distributed randomly on the lattice sites and (b) the oxygen defect appears between two copper sites when it is linked to two adjacent Sr^{2+} ions as in Sr_2CuO_3 .¹⁵ Although the simulation does not take into account any dependence on the partial pressure of oxygen, we find that stoichiometric compounds are formed at low values of x and oxygen defects become appreciable when $x > 0.30$ (Fig. 3), in agreement with our experimental results. At low values of Sr concentrations, the probability of two Sr ions coming adjacent to each other is small, hence stoichiometric compounds are formed in this limit. An increase in this probability at higher Sr concentrations, increases the oxygen defect concentration. The agreement of the simulated result with experiment suggests that the loss of oxygen takes place from the a - b plane as Cu- V -Cu (V indicates an oxygen vacancy) similar to that of Sr_2CuO_3 . The data of Nguyen *et al.*⁸ show that the Sr_2CuO_3 phase, in fact, separates out when $x > 1.33$. This model therefore supports the localization of oxygen vacancies in the a - b plane,⁸ as evidenced by the

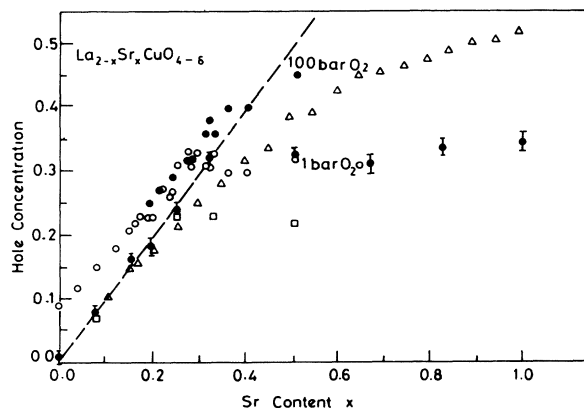


FIG. 3. Evolution of the hole concentration as a function of x in the $\text{La}_{2-x}\text{Sr}_x\text{CuO}_{4-\delta}$ system. The open and solid circles are from Ref. 9, the open squares from Ref. 8, and the open triangle gives the simulated result as described in the text.

electron diffraction studies (Fig. 4). In fact, the ability of a Cu^{2+} ion to take different coordination number and geometries plays an important role in stabilizing the oxygen defect structures in these systems.

The observed “intercalation” and “disintercalation” of oxygen in these systems can be accounted for by the relative change in the crystal-field splitting, and hence the change in the d -orbital energies, as a function Cu—O bond distance. In the $\text{La}_{2-x}\text{Sr}_x\text{CuO}_{4-\delta}$ system the “intercalation” of oxygen takes place in the basal plane. The Cu^{2+} ion has its one unpaired electron in the energetically unfavorable $d_{x^2-y^2}$ orbital in the elongated octahedral or square-planar geometry. On oxidation, or “intercalation” of oxygen in the basal plane, the a parameter decreases and the Cu-O hybridization increases. The resultant increase in the crystal-field splitting destabilizes the unpaired electron in the $d_{x^2-y^2}$ orbital, which facilitates the metal to ligand charge transfer to form low-spin Cu^{3+} ions.¹⁶ In the reverse process, the reduction or “disintercalation” of oxygen from the basal plane, stabilizes the $d_{x^2-y^2}$ orbital which favors the ligand to metal charge transfer and the formation of Cu^{2+} ions.

B. Structural properties

The lattice parameters, c/a ratio, and the molar volume of the series $\text{La}_{2-x}\text{Sr}_x\text{CuO}_{4-\delta}$ ($0.0 \leq x \leq 1.2$) are plotted in Figs. 5 and 6, respectively. The lattice parameters of the compounds obtained by us are in good agreement with those reported earlier.^{8,10} In the range $0.0 < x < 0.33$ the c parameter increases gradually while the a parameter shows a decrease. The samples annealed in 1 bar oxygen show a maximum in the c/a ratio⁸⁻¹⁰ around the composition $x = 0.33$, up to which there is no oxygen deficiency. For a given value of x , the c parameter decreases on the removal of oxygen. When $x > 0.33$ both the a and c parameters decrease. The decrease in the c parameter is found to be large compared to that of the a parameter.

The most revealing change in the structural feature with an increase in x is the increase in the c/a ratio observed in the range $0.0 < x < 0.33$ where there is no oxygen deficiency. The increase in the c/a ratio with x in this range is dependent on two factors: (i) the relative size of the substituent ions and (ii) the change in the Cu—O network in going from Cu^{2+} ions to low-spin Cu^{3+} ions. The substitution of La^{3+} ions by a slightly larger Sr^{2+} ions increases the c parameter, but the a parameter is affected little since it is determined by the Cu—O bond distance in the a - b plane. The second factor is the formation of low-spin Cu^{3+} ions by the substitution of divalent Sr^{2+} ions for trivalent La^{3+} ions for charge balance in the stoichiometric compounds. The Cu^{3+} ions are known to be stable in square-planar or elongated octahedral geometry.^{17,18} Their metal-ligand bond distances in the basal plane are short compared to the corresponding Cu^{2+} compounds.¹⁶ Thus, the oxidation of Cu^{2+} to Cu^{3+} decreases the a parameter (Cu—O bond distance in the a - b plane) and increases the c parameter (Cu—O bond length along the c axis) which increases the c/a ratio. In La_4LiBO_8 ($B = \text{Co}, \text{Ni}, \text{and Cu}$) the c/a ratio is

largest when $B = \text{Cu}^{3+}$ ion.¹⁸ The increase in the c/a ratio found by substituting Ca^{2+} ions,⁸ which have a smaller ionic radius than La^{3+} ions, in the $\text{La}_{2-x}\text{Ca}_x\text{CuO}_4$ samples indicate that the second factor dominates over the first one in these systems.

Moreover, the lattice parameters of the $\text{La}_{2-x}\text{Sr}_x\text{CuO}_{4-\delta}$ system do not obey Vegard's law¹⁹ of solid solution even in the limited range $0.0 \leq x \leq 0.33$

where there is no oxygen vacancy. This also suggests that the electronic factors, for instance the change of valence of copper, play a dominant role in determining the nature of the Cu-O network on Sr substitution. In this respect the creation of Cu^{3+} decreases the a parameter and increases the c parameter which increases the c/a ratio. The percentage change in the a parameter is also consistent with the creation of the hole on copper when

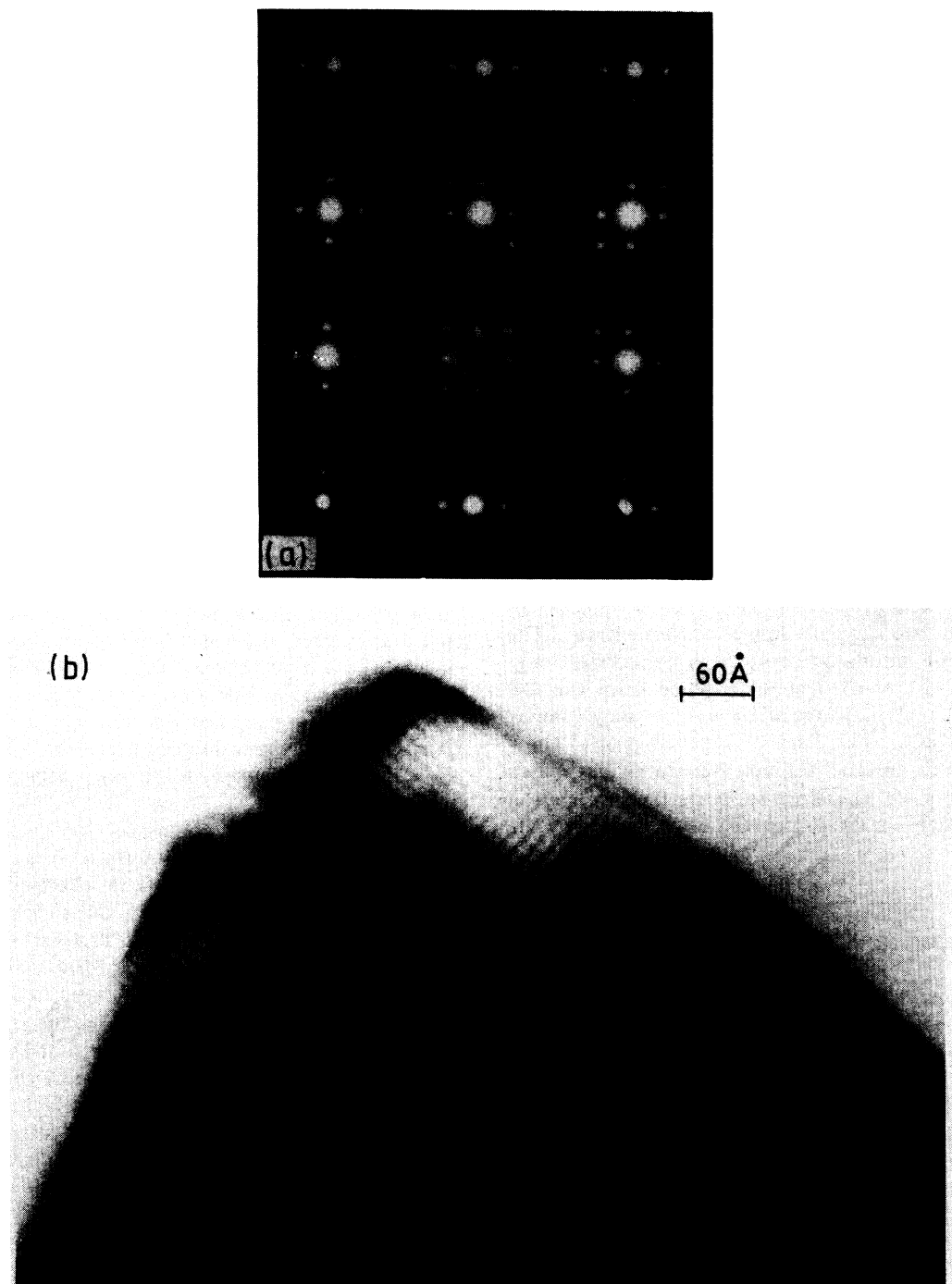


FIG. 4. Typical electron diffraction pattern (a) and lattice image (b) obtained for the $x = 1.2$ sample along the $[001]$ direction showing $(5 \times)$ a K_2NiF_4 superlattice and $\sim 18 \text{ \AA}$ fringes.

we compare the Shannon-Prewitt radii²⁰ for Cu^{2+} and Cu^{3+} ions. The minimum in the molar volume around $x=0.15$ indicates that the decrease in the a parameter dominates more than the increase in the c parameter up to this composition.

The decrease in the c/a ratio for $x > 0.33$ is to be associated with the formation of oxygen vacancies. For the samples annealed at an oxygen pressure of 100 bar, the oxygen vacancies appear only above $x=0.40$ and the c/a ratio increases up to $x=0.40$ and then it decreases.⁹ The $x > 0.66$ samples have a c/a ratio less than that of La_2CuO_4 itself but greater than that of Sr_2CuO_3 [Sr_2CuO_3 has an orthorhombic structure,¹⁵ so for comparison we define c/a as $2c/(a+b)$]. With the increase of oxygen vacancies, the coordination number around Cu^{2+} ion changes from 6 to 5 and then to 4. This changes the coordination geometry around the Cu^{2+} ion from elongated octahedra to square pyramidal and eventually to square planar. This results in a change in the orbital ordering like that in Sr_2CuO_3 , which decreases the Cu—O bond distance along the c axis from ~ 2.4 Å observed in the CuO_6 octahedral geometry²¹ of La_2CuO_4 to ~ 1.96 Å in the square-planar geometry¹⁵ of Sr_2CuO_3 . The loss

of oxygen from the basal plane can also increase the axial Cu—O₂ interaction along the c axis and decrease the c parameter.

C. Infrared transmission studies

1. Studies with model compounds

The infrared (ir) transmission spectral features of structurally related copper oxides such as Ca_2CuO_3 ,²² $\text{La}_4\text{LiCuO}_8$,¹³ $\text{Sr}_2\text{CuO}_2\text{Cl}_2$,²³ and Nd_2CuO_4 (Ref. 24) are shown in Fig. 7, with special reference to the stretching frequency versus Cu—O bond distance. The infrared spectra²⁵ of a variety of copper oxides with different Cu—O distances (MgCu_2O_3 , $\text{Ba}_2\text{C}_3\text{O}_4\text{Cl}_2$, Bi_2CuO_4 , and Y_2BaCuO_5) shows that the highest-frequency ir band in these copper oxide compounds seems to be inversely related to the short Cu—O bond distance (Fig. 8). For instance, La_2CuO_4 , Ca_2CuO_3 , and $\text{La}_4\text{LiCuO}_8$, which have short Cu—O bond distances^{21,22,13} (< 1.90 Å), show a high-frequency band around $670\text{--}690\text{ cm}^{-1}$. This high-frequency band is absent in compounds such as Sr_2CuO_3 , $\text{Sr}_2\text{CuO}_2\text{Cl}_2$, and Nd_2CuO_4 with longer Cu—O bond dis-

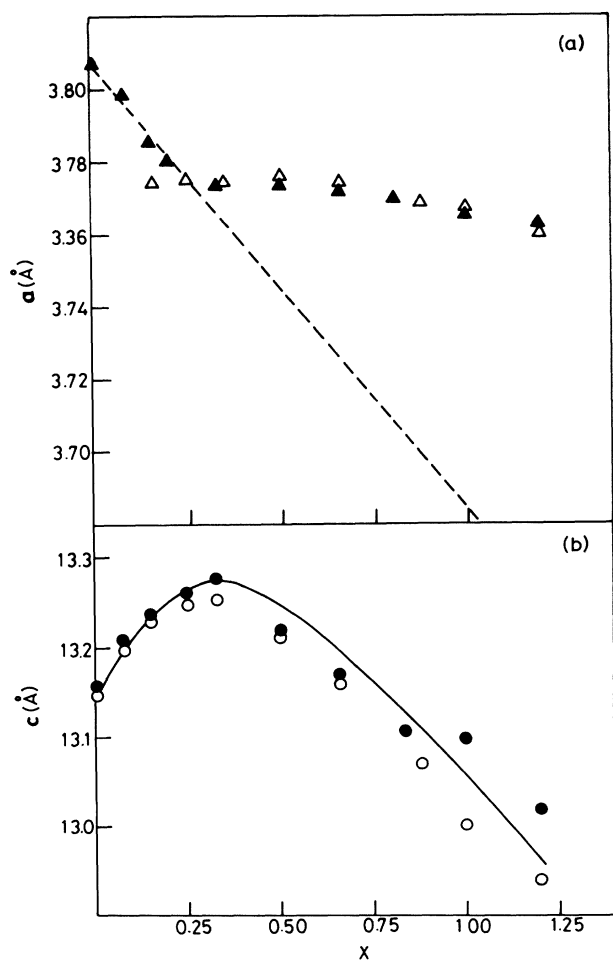


FIG. 5. Variation of the a (a) and c parameters as a function of x for the $\text{La}_{2-x}\text{Sr}_x\text{CuO}_{4-\delta}$ system. [The open triangles in (a) and open circles in (b) are from Ref. 8].

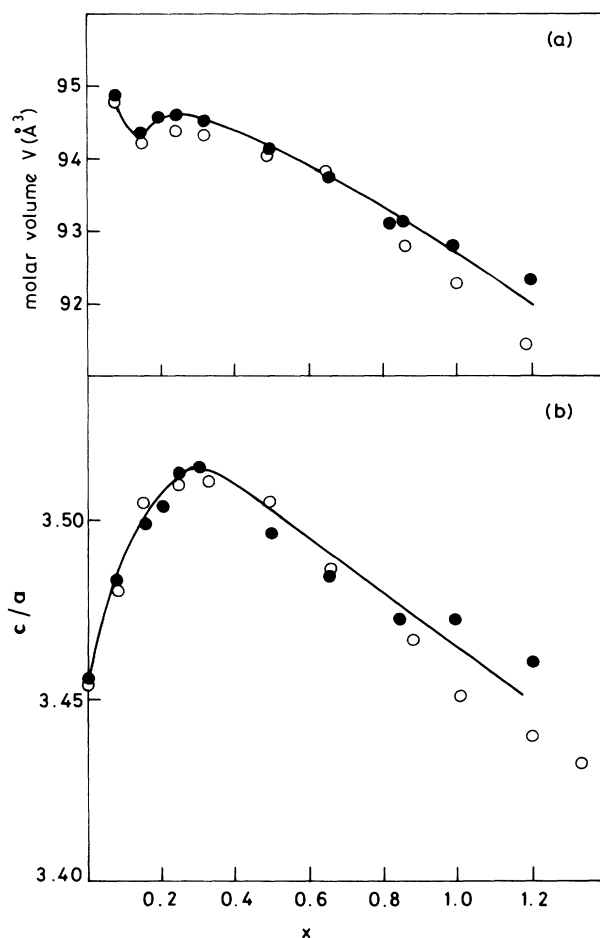


FIG. 6. Evolution of the molar volume (a) and the change in the c/a ratio (b) as a function of x in the $\text{La}_{2-x}\text{Sr}_x\text{CuO}_{4-\delta}$ system (the open circles are from Ref. 8).

tances.^{15,23,24} We also note that the highest ir stretching frequency of the $\text{La}_4\text{LiCuO}_8$ having a short Cu—O bond distance of $\sim 1.865 \text{ \AA}$ is higher than that of La_2CuO_4 which has a relatively long Cu—O bond distance $\sim 1.90 \text{ \AA}$. This suggests that an increase in the force constant with the decrease in the Cu—O bond distance shifts the ir stretching frequency to higher values.

2. $\text{La}_{2-x}\text{Sr}_x\text{CuO}_{4-\delta}$ system

We have studied the changes in the infrared spectra of the compound $\text{La}_{2-x}\text{Sr}_x\text{CuO}_{4-\delta}$ as a function of x ($0.0 \leq x \leq 1.2$). The infrared spectra in the region $1000\text{--}300 \text{ cm}^{-1}$ of these compounds are shown in Figs. 9 and 10. The $x=0.0$ sample shows three ir bands at 675 , 510 , and the 360 cm^{-1} . In the range ($0.08 \leq x \leq 0.20$) the high-frequency 675 cm^{-1} band disappears (Fig. 14) and the two low-frequency (510 and 360 cm^{-1}) ones survive. All the ir bands disappear on further increase in x ($0.25 < x < 0.50$). When $x > 0.5$, the infrared bands reappear. What is interesting is the reappearance of all the ir bands, including the high-frequency band around 675 cm^{-1} for the $x=0.66$ sample, which show metallic electrical resistivity behavior. But the frequency of these

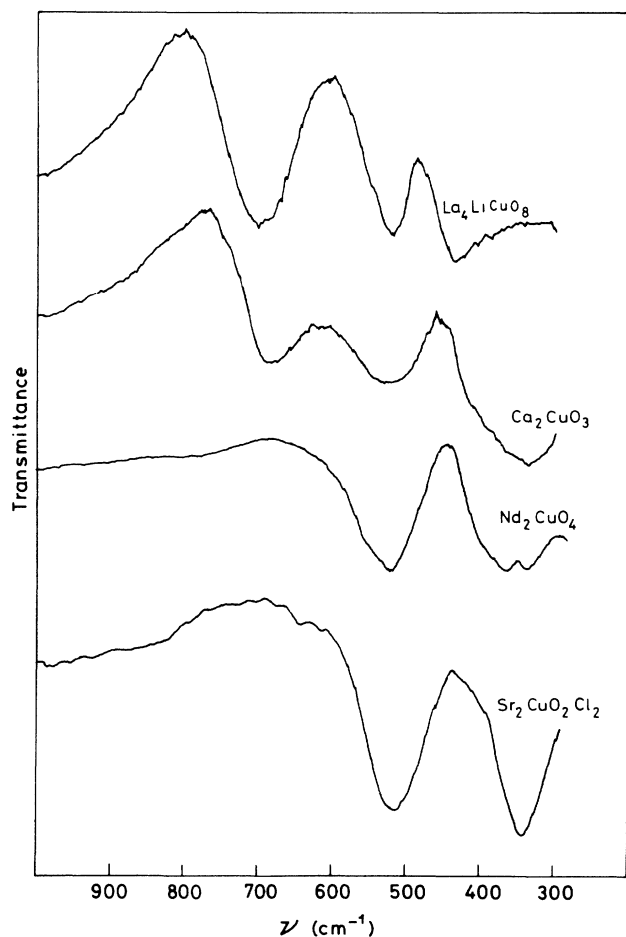


FIG. 7. Infrared absorption spectra of some model copper compounds related to K_2NiF_4 structure with different Cu—O distances.

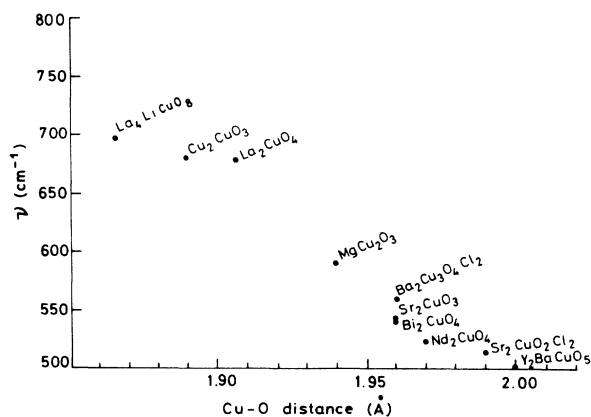


FIG. 8. Variation of the highest Cu—O stretching frequency with Cu—O bond distance in some model copper compounds.

bands does not change much in the range $0.5 < x < 0.83$. For $x > 0.83$ the frequency of the band around 670 cm^{-1} decreases with increasing x while the frequency of the band around 510 cm^{-1} increases with increasing x .

In the $\text{La}_{2-x}\text{Sr}_x\text{CuO}_{4-\delta}$ system the high-frequency band around 675 cm^{-1} has been assigned to an in-plane stretching E_u mode where the Cu—O distance is short,

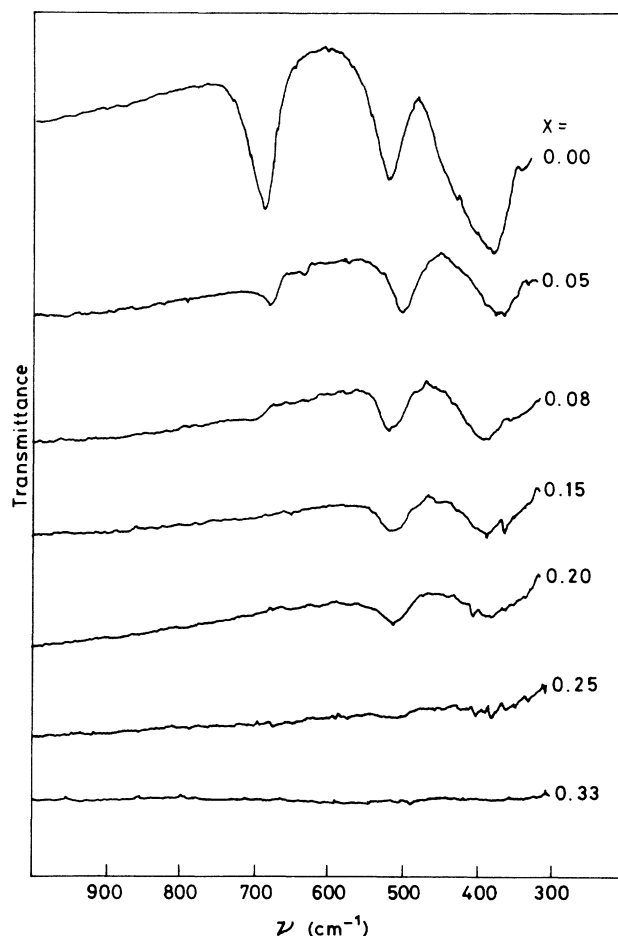


FIG. 9. Evolution of the ir spectrum as a function of different Sr concentrations in the range ($0.0 < x < 0.33$).

while the other low-frequency bands around 510 and 360 cm^{-1} could correspond to an out-of-plane A_{2u} stretching mode.²⁶ The disappearance of the 675 cm^{-1} band in the $\text{La}_{2-x}\text{Sr}_x\text{CuO}_4$ system in the range ($0.05 < x < 0.20$) can then be attributed to the metallization in the a - b plane since the free electron couples more to the E_u modes than to the A_{2u} modes. In this interpretation, the 510 and 360 cm^{-1} bands which survive in the superconducting $x=0.15$ and 0.20 samples could be attributed to the out-of-plane A_{2u} modes since the compounds show insulating behavior perpendicular to the a - b plane. Single-crystal studies on La_2CuO_4 show the 360 cm^{-1} band to have a polarization in the a - b plane.²⁷ The persistence of this band in the superconducting samples would then suggest that the 360 cm^{-1} band could be associated with the in-plane La-O_2 stretching mode²⁸ in the insulating La-O_2 layers.

The disappearance of both the in-plane and out-of-plane infrared absorption bands for the $x=0.33$ composition is reminiscent of the disappearance of all the infrared absorption bands in the metallic side of the Insulator-Metal transition boundary^{29,30} of the three-dimensional perovskites. The disappearance of high- T_c superconductivity around this composition may then be linked to such isotropic band metallization.

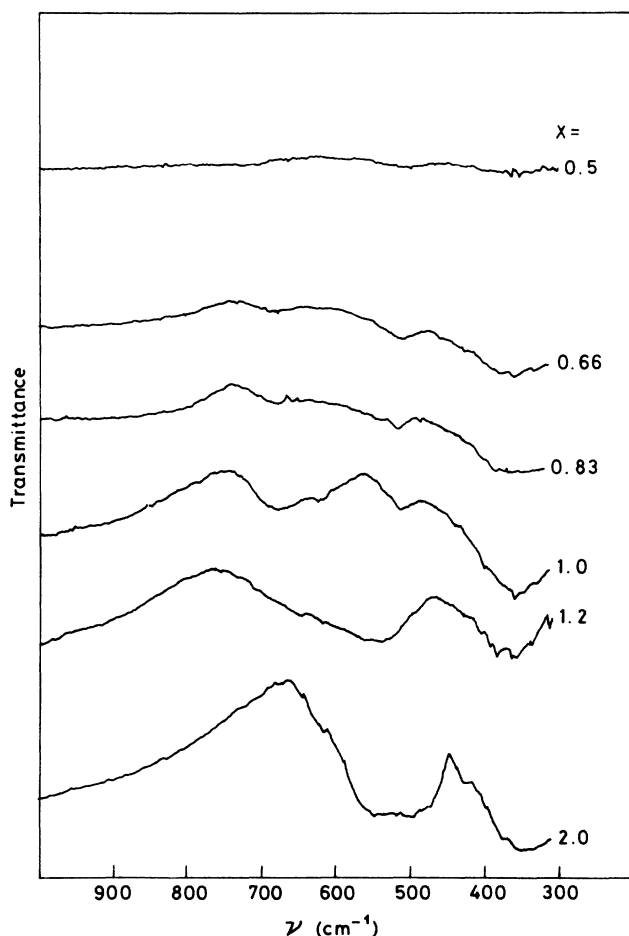


FIG. 10. Evolution of the ir spectrum as a function of x in the range ($0.5 < x < 2.0$).

The survival of all the ir bands, including the band around 675 cm^{-1} for $x=0.66$ composition which shows a metallic electrical resistivity behavior, would suggest a compositional as well as an oxygen inhomogeneity. This can result in the formation of La-rich metallic and oxygen deficient Sr-rich insulating regions within the K_2NiF_4 -type structure. Such a compositional inhomogeneity seems possible since the compound can exist in a wide composition range with varying oxygen content in the K_2NiF_4 -type structure, with close thermodynamic stability.

The observed broadening and shifting of the ir bands at higher Sr concentrations $x > 0.66$ indicate the possibility of different local coordinations for copper. With increasing x the highest-frequency band shifts to lower values despite a decrease in the a parameter. This behavior can be qualitatively understood if we assume that the oxygen vacancies are distributed randomly in the a - b plane, so that overall one obtains a tetragonal structure. This behavior is similar to the tetragonal $\text{LnBa}_2\text{Cu}_3\text{O}_{7-\delta}$ compounds which have the oxygens disordered in the a - b plane. The Cu-V-Cu distance is expected to be smaller than the Cu-O-Cu distance as observed in Sr_2CuO_3 .¹⁵ An increase in Cu-O distance in the basal plane decreases the stretching frequency, but the simultaneous increase in the number of oxygen vacancies at higher values of x decreases the overall a parameter. The decrease in the frequency would then be similar to that observed on going from Ca_2CuO_3 with short Cu-O distance to Sr_2CuO_3 with long Cu-O distance.

D. Magnetic susceptibility studies

We have carried out a magnetic susceptibility study on the oxygen annealed samples in the range ($0.0 \leq x \leq 1.2$). The magnetic susceptibility of La_2CuO_4 ($x=0.0$) is small³¹ ($\sim 0.5\mu_B$ at 300 K) and weakly temperature dependent at high temperatures. But at low temperatures the susceptibility shows a relatively large temperature dependence. The temperature dependence of the susceptibility shows a maximum around 250 K (Ref. 32) which has been attributed to three-dimensional antiferromagnetic ordering³³ and has been confirmed by neutron diffraction studies.³¹ It is known that as the Sr concentration increases, the long-range antiferromagnetic order rapidly disappears³⁴ and it becomes "Pauli" paramagnetic. The $x=0.0$ sample shows a strong field dependence in the susceptibility which persists until high temperatures. The field dependence has also been observed in single-crystal studies on La_2CuO_4 .³⁵

1. $0.08 < x < 0.33$

The temperature variation of the magnetic susceptibility of some members of the $\text{La}_{2-x}\text{Sr}_x\text{CuO}_4$ series ($0.0 \leq x \leq 0.33$) are shown in Fig. 11. The magnitude of the susceptibility at 300 K shows a maximum around $x=0.15$ and a minimum around 0.33 (Fig. 11 inset). No field dependence has been observed in the $x > 0.15$ sam-

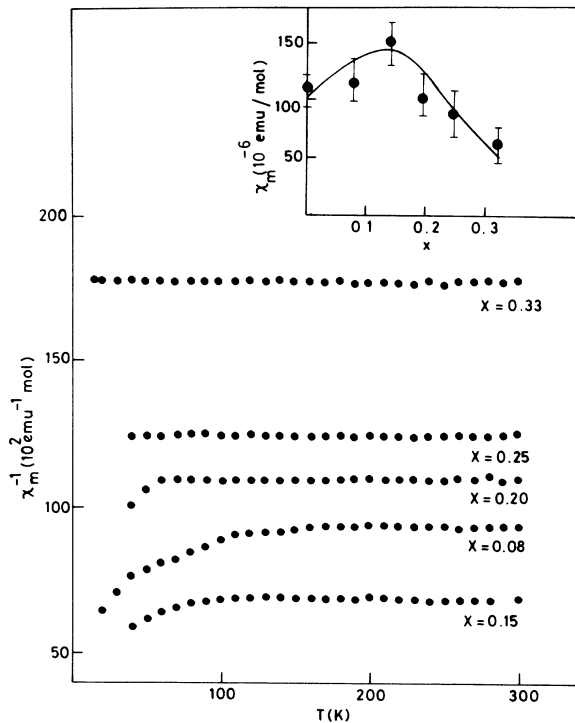


FIG. 11. Temperature dependence of the inverse magnetic susceptibility for different Sr concentrations x in the range ($0.0 < x < 0.33$). The inset shows the variation of the Pauli magnetic susceptibility as a function of x at 300 K.

ples. In the range $0.08 \leq x \leq 0.20$ the compounds show a weak temperature dependence in the susceptibility at low temperatures, like that of the parent compound La_2CuO_4 . The onset of the temperature dependence shifts to lower temperatures as x increases. When $x > 0.20$ the susceptibility becomes temperature independent (true Pauli type) down to 14 K. Even though the Pauli susceptibility increases with x up to $x = 0.15$, a significant decrease in the magnitude of the Pauli susceptibility has been observed when $x > 0.15$. In fact, the magnitude of the Pauli susceptibility of the $x = 0.33$ sample is $\sim 58 \times 10^{-6}$ emu/mol at 300 K. This is only half of the observed Pauli susceptibility of the $x = 0.15$ composition. Moreover, the samples in the range $0.15 \leq x \leq 0.20$ have the highest Meissner fraction at 14 K with an onset of a diamagnetic contribution below 36 K (Fig. 12). The onset of the Meissner effect close to 36 K (Ref. 9) and a decrease in the Meissner fraction³⁶ with increasing x in the range $0.15 \leq x \leq 0.25$ suggest a compositional inhomogeneity which is similar to that observed in the superconducting $\text{Li}_{1+x}\text{Ti}_{2-x}\text{O}_4$ system.³⁷

The observed increase in the Pauli magnetic susceptibility with x in the range $0.08 \leq x \leq 0.15$, and the enhancement of the Pauli susceptibility at low temperatures is similar to that observed in the case of $\text{YBa}_2\text{Cu}_3\text{O}_{7-\delta}$ samples in the range $0.0 < \delta < 0.5$.³⁸ This enhancement of the Pauli susceptibility can be attributed to the presence of highly correlated charge carriers in a narrow d band.^{20,39} The temperature dependence of the thermopower^{10,40} at this composition range is also consistent with strongly correlated charge carriers. But the

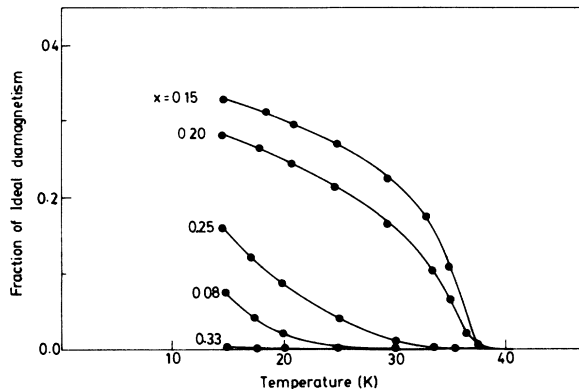


FIG. 12. Variation of the percentage Meissner fraction obtained at a field of 500 G for the $\text{La}_{2-x}\text{Sr}_x\text{CuO}_4$ ($0.08 < x < 0.33$) system.

observed decrease in the magnitude of Pauli susceptibility relative to the $x = 0.15$ composition by half in the metallic $x = 0.33$ sample could be attributed to a transition from a highly correlated narrow-band Mott-conducting regime to a broadband metal. This transition from a highly correlated narrow-band metal to a broadband metal occurring at this composition ($x = 0.33$) decreases the density of states (DOS) at E_F which decreases the Pauli magnetic susceptibility. In fact, this transition occurring at $x = 0.33$ suppresses the superconductivity down to 4.2 K in this system.

2. $0.5 \leq x \leq 1.2$

All these samples show a temperature-dependent Curie-type susceptibility below room temperature (Fig. 13). The temperature dependence and the C value in-

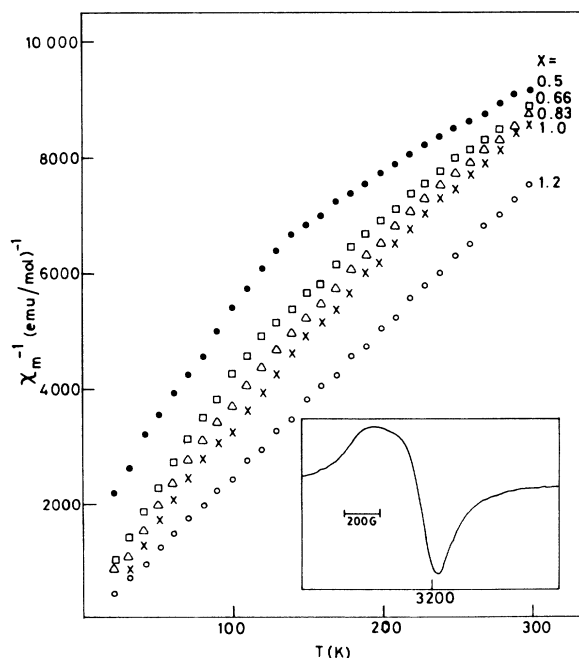


FIG. 13. Temperature dependence of the inverse magnetic susceptibility for the range $0.50 < x < 1.2$. The inset shows the EPR spectrum of the $x = 1.2$ sample at 300 K.

crease with increasing x (Table I). The susceptibility behavior can be expressed in terms of an expression of the type $X = (C/T) + m$, where the values of C and m determine the temperature-dependent Curie-type susceptibility and temperature-independent Pauli susceptibility, respectively. The values of C and m , which give the best fit for our data, are given in Table I. The value of C goes through a minimum around $x = 0.33$ and the value of m shows a maximum around $x = 0.15$ – 0.20 . When $x > 0.33$ the magnitude of C increases with increasing x and reaches 0.04 emu K/mol for the $x = 1.2$ sample. In fact, there is a direct correlation between the d and C values which increases with an increase in d . The EPR studies on these samples show a signal characteristic of Cu^{2+} ions in square-planar coordination (Fig. 13 inset). The concentration of isolated Cu^{2+} spins calculated from the integrated intensity of the EPR signal agrees well with the C value obtained from the magnetic susceptibility studies. This is consistent with the creation of isolated Cu^{2+} ions due to the creation of oxygen vacancies in the Cu-O plane. But the large reduction in the magnitude of the susceptibility, from that expected for an $S = \frac{1}{2}$ system, can be attributed to the existence of a high antiferromagnetic correlation due to the 180° Cu-O-Cu superexchange interaction as observed in Ca_2CuO_3 , Sr_2CuO_3 , and other ternary copper oxides.⁴¹

E. Electrical transport properties

We have studied the electrical transport properties of the $\text{La}_{2-x}\text{Sr}_x\text{CuO}_{4-\delta}$ ($0.0 \leq x \leq 1.2$) system down to 14 K. The $x < 0.05$ samples are not superconducting down to 14 K. Superconducting transitions were observed in the range $0.08 \leq x \leq 0.25$. T_c shows a maximum (36 K) around $x = 0.15$ (Fig. 14). In the composition range $0.33 \leq x \leq 0.66$ the compounds show a positive temperature coefficient of resistivity typical of a normal metal (Fig. 14). A linear temperature dependence of resistivity has been observed in all the metallic samples down to 14 K. In the Bloch-Gruneisen form for resistivity, deviation from linear behavior occurs below $T \sim 0.5\Theta_D$ (the Debye temperature). Hence, a Debye temperature of ~ 300 – 400 K for these systems⁴² may suggest that the Bloch-Gruneisen behavior is not valid in these metallic low-dimensional copper oxide systems. But it is interesting to

TABLE I. Magnetic susceptibility data for the $\text{La}_{2-x}\text{Sr}_x\text{CuO}_{4-\delta}$ system for different x values at 300 K.

x	C (emu K mol ⁻¹)	m (10^{-6} emu mol ⁻¹)
0.08	0.001	105
0.15	0.0005	145
0.20		90
0.25		80
0.33		58
0.50	0.008	85
0.66	0.020	45
0.83	0.024	35
1.00	0.030	5
1.20	0.040	

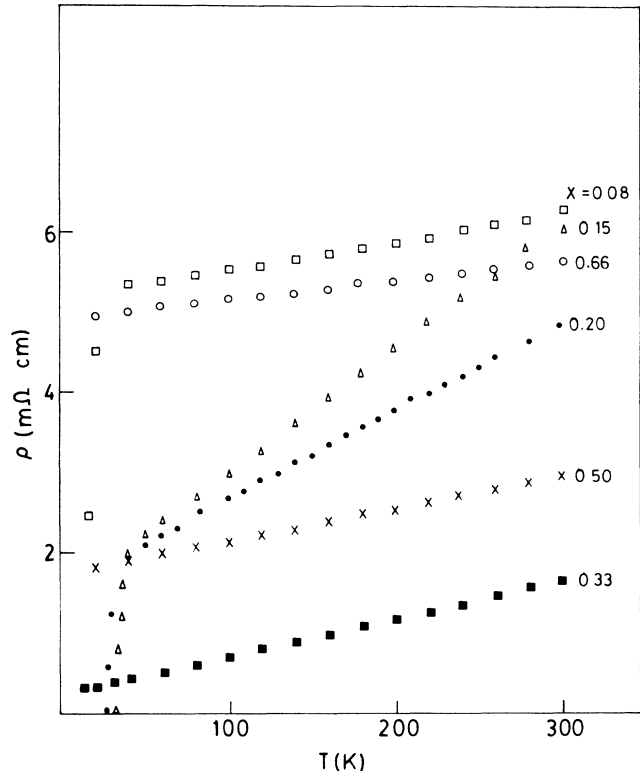


FIG. 14. Temperature variation of the electrical resistivity for the samples with different Sr concentrations in the range ($0.08 < x < 0.66$).

note that the temperature-dependent electrical resistivity of the three-dimensional metallic perovskite $\text{La}_4\text{BaCu}_5\text{O}_{13+\delta}$ shows a deviation from linearity^{43,6} below 100 K. At higher values of x ($0.66 < x \leq 1.2$) the compounds show semiconducting resistivity behavior with a pronounced negative temperature coefficients of resistivity (TCR) (Fig. 15). The TCR changes sign when the value of the resistivity reaches $\sim 2 \times 10^{-3}$ ohm cm. This is the value at which the TCR changes sign in most of the oxide systems undergoing an insulator-metal transition.⁴⁴

The electrical transport properties of these copper oxide systems can be rationalized in terms of large U . The parent compound La_2CuO_4 having Cu^{2+} ions in the elongated octahedral symmetry of the oxide ligands, has one unpaired electron in the $3d_{x^2-y^2}$ orbital which is hybridized with the $\text{O}:2p_{x,y}$ orbitals and the band is half-filled. If the on-site Coulomb correlation U is large compared with the bandwidth (zt), where z and t are the coordination number and the transfer integral, respectively, the originally half-filled antibonding ($\text{Cu}:3d_{x^2-y^2} - \text{O}:2p_{x,y}$) band of the parent compound La_2CuO_4 splits into lower (full) and upper (empty) Hubbard bands with a Coulomb gap and it is in the Mott-Hubbard insulating limit. At a low level of Sr doping ($0.08 \leq x \leq 0.2$), holes are created in the lower Hubbard band which are itinerant and it becomes metallic. But the persistence of a Coulomb gap in the c direction at this doping range can account for the high anisotropy in the transport properties and the two-dimensional metallization. An increase

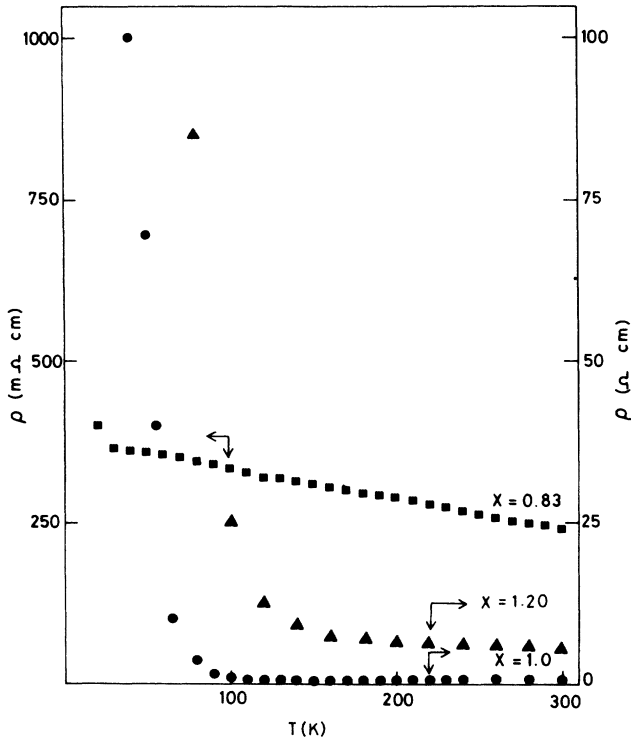


FIG. 15. Temperature variation of the electrical resistivity for the samples with different Sr concentrations x in the range ($0.83 < x < 1.20$).

in the number of holes as well as the transfer integral (due to the decrease in the a parameter) at high Sr concentrations ($0.15 \leq x \leq 0.33$) increases the bandwidth and the Coulomb gap can vanish altogether and it can become a quasi-three-dimensional band metal around the composition $x = 0.33$ (Fig. 16). The T_c also decreases with x in this range and the superconductivity vanishes around the composition $x = 0.33$ where a possible electronic dimensionality crossover occurs. We have confirmed the vanishing of superconductivity at this composition down to 4.2 K.

The observed increase in resistivity ($x > 0.33$) and the

semiconducting resistivity behavior ($x > 0.66$) at higher Sr concentrations is consistent with the localization of charge carriers due to oxygen vacancies. The creation of oxygen vacancies in the a - b plane induce disorder and when it exceeds a certain critical value the carriers become localized.⁴⁵ This critical disorder seems to occur around $x \sim 0.66$ in this system. The observed semiconducting behavior for $x > 0.66$ samples and the absence of superconductivity in this composition region could then be associated with the strong localization effect due to the creation of oxygen vacancies in the a - b plane which destroys metallicity and superconductivity.

IV. GENERAL REMARKS

We have summarized our results on the electrical transport properties of the $\text{La}_{2-x}\text{Sr}_x\text{CuO}_{4-\delta}$ system in Fig. 17. The electrical resistivity data of the parent compound La_2CuO_4 ($x = 0$) has been rationalized in terms of an antiferromagnetic Mott-Hubbard insulator,⁴⁶ with a correlation gap. Although polycrystalline La_2CuO_4 shows semiconducting resistivity behavior, the single crystals show high anisotropy in the resistivity. Perpendicular to the a - b plane it has a semiconducting resistivity behavior but the samples having a resistivity ~ 0.1 ohm cm show metallic resistivity behavior along the a - b plane.⁴⁷ This would then mean that the temperature dependence of the electrical resistivity in these low-dimensional polycrystalline samples are affected by the high anisotropy in the conductivity.

A linear increase in the number of charge carriers observed by Hall-effect measurements⁴⁸⁻⁵⁰ in the range $0.0 \leq x \leq 0.15$ has been attributed to the presence of a Coulomb gap at the Fermi level.⁴⁸ Our magnetic susceptibility, electrical resistivity, and particularly, infrared results support such an interpretation. A linear increase in T_c with hole concentration is valid only in the range ($0.0 < x < 0.15$) where there is a Coulomb gap at E_F . The disappearance of this Coulomb gap at a high-hole concentration can affect the nature of electronic conduction and drives the system to a nonsuperconducting metallic phase.

Hence, the disappearance of high- T_c superconductivity

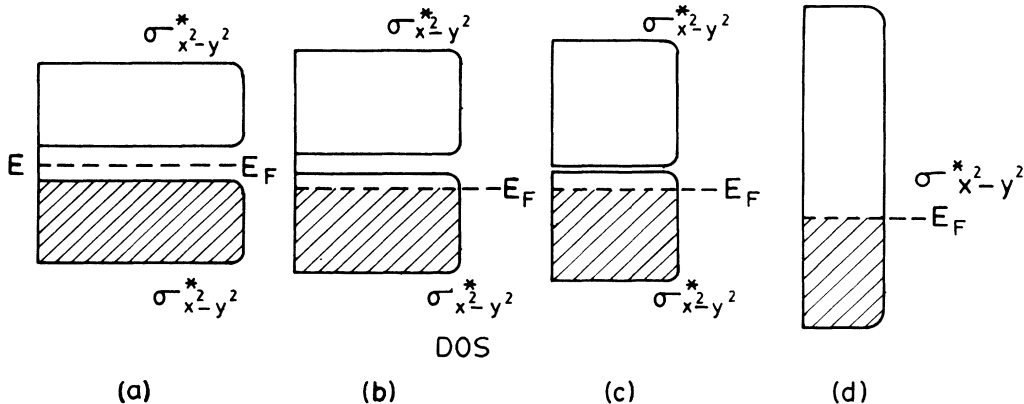


FIG. 16. Schematic band diagram proposed for the $\text{La}_{2-x}\text{Sr}_x\text{CuO}_4$ system. (a) $x = 0.0$, (b) $x = 0.15$, (c) $x = 0.20$, and (d) $x = 0.33$.

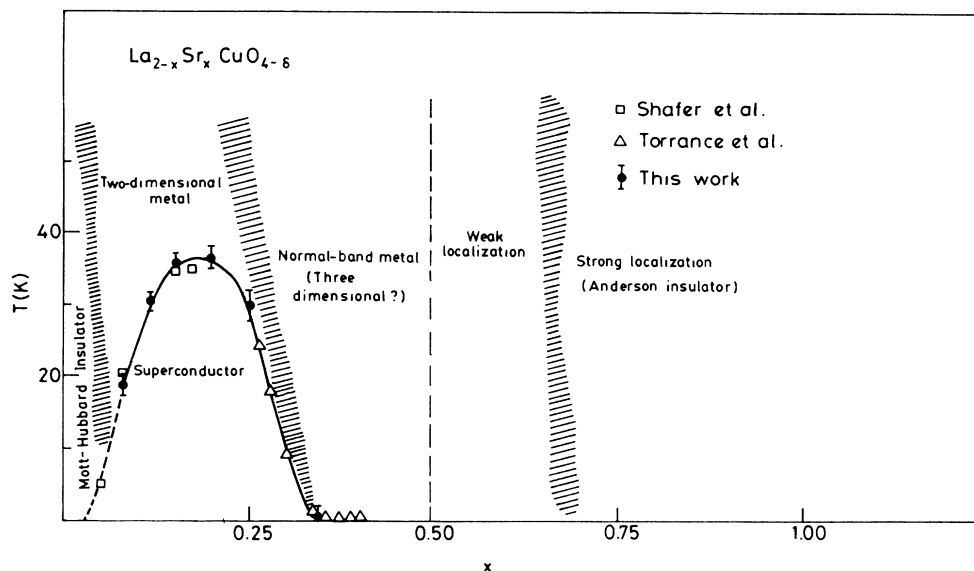


FIG. 17. Schematic phase diagram describing the electrical transport properties of the $\text{La}_{2-x}\text{Sr}_x\text{CuO}_{4-\delta}$ ($0.0 < x < 1.20$) system.

at high-hole concentrations could be associated with a change in the nature of electronic conduction, namely, from a highly correlated “Mott conductor” (at low-hole concentrations) to a broadband metal (at high-hole concentrations) due to the band broadening effects and the concomitant vanishing of the Coulomb gap. This disappearance of the Coulomb gap in the c direction can possibly also lead to a dimensional crossover from two-dimensional to quasi-three-dimensional metallization which suppresses the T_c . A rapid decrease in the Hall coefficient^{48–49} R_H above $x > 0.15$, decrease in the magnitude of room-temperature resistivity, Pauli magnetic susceptibility, and the disappearance of all the ir bands around $x = 0.33$ are typical of the behavior expected for a broadband three-dimensional metal. This suggests that although the system preserves a two-dimensional lattice for a wide composition range⁸ ($0.0 < x < 1.33$), a change in the carrier concentration, transfer integral, and electron-electron correlation, etc., can change the electronic structure as well as the topology of the Fermi surface which changes the electrical transport in these systems. The absence of high- T_c superconductivity⁶ in some of the metallic copper oxides which does not have a low-dimensional structure ($\text{La}_{2-x}\text{Sr}_{1+x}\text{Cu}_2\text{O}_{6+\delta}$ and $\text{La}_4\text{BaCu}_5\text{O}_{13+\delta}$) also suggests the importance of low-dimensional electronic structure for high- T_c supercon-

ductivity in these systems. The increase in resistivity, increase in Curie constant, and reappearance of all the ir bands at higher values of x ($0.5 \leq x \leq 1.20$) which have relatively high-hole concentrations ($\sim 30\%$) suggest disorder-induced localization due to the creation of oxygen vacancies.

In conclusion, our results on $\text{La}_{2-x}\text{Sr}_x\text{CuO}_{4-\delta}$ suggest that a linear increase in T_c with hole concentration is valid as long as the system has a two-dimensional character. The disappearance of high- T_c superconductivity in the metallic, stoichiometric samples with high-hole concentrations is related to the transition from a highly correlated “Mott conductor” to a broadband metal due to the disappearance of the Coulomb gap. This can also possibly change the anisotropic two-dimensional transport and the system can become a quasi-three-dimensional metal. Disorder-induced localization of charge carriers is observed at higher Sr concentrations due to the creation of oxygen vacancies in the Cu-O plane.

ACKNOWLEDGMENTS

The authors are thankful to Dr. N. Y. Vasanthacharya and Dr. K. P. Rajeev for their help in the resistivity measurements of one of our samples down to 4.2 K. One of us (K.S.) is grateful to the University Grants Commission, India for partial financial support.

¹J. G. Bednorz and K. A. Muller, *Z. Phys. B* **64**, 189 (1986).

²(a) S. Uchida, H. Takagi, K. Kitazawa, and S. Tanaka, *Jpn. J. Appl. Phys.* **26**, L1 (1987); (b) H. Takagi, S. Uchida, K. Kitazawa, and S. Tanaka, *ibid.* **26**, L123 (1987); (c) C. W. Chu, P. H. Hor, R. L. Meng, L. Gao, Z. J. Huang, and Y. Q. Wang, *Phys. Rev. Lett.* **58**, 405 (1987).

³M. K. Wu, J. R. Ashburn, C. J. Torng, P. H. Hor, R. L. Meng, L. Gao, J. Huang, Y. Q. Wang, and C. W. Chu, *Phys. Rev. Lett.* **58**, 908 (1987); (b) R. J. Cava, R. B. VanDover, B.

Batlogg, and E. A. Rietman, *ibid.* **58**, 408 (1987); (c) R. J. Cava, B. Batlogg, R. B. VanDover, D. W. Murphy, S. Sunshine, T. Siegrist, J. P. Remeika, E. A. Rietman, S. Zahurak, and G. P. Espinosa, *ibid.* **58**, 1676 (1987); (d) C. N. R. Rao, P. Ganguly, A. K. Raychaudhuri, R. A. Mohan Ram, and K. Sreedhar, *Nature* **326**, 856 (1987); (e) P. Ganguly, R. A. Mohan Ram, K. Sreedhar, and C. N. R. Rao, *Pramana*, *ibid.* **28**, L321 (1987).

⁴(a) C. Michel, M. Hervieu, M. M. Borel, A. Grandin, F.

- Deslandes, J. Provost, and B. Raveau, *Z. Phys. B* **68**, 412 (1987); (b) A. H. Maeda, Y. Tanaka, N. Fukutomi, and T. Asano, *Jpn. J. Appl. Phys.* **27**, L209 (1988); (c) C. W. Chu, J. Bechtold, L. Gao, P. H. Hor, Z. J. Huang, R. L. Meng, Y. Y. Sun, Y. Q. Wang, and Y. Y. Xue, *Phys. Rev. Lett.* **60**, 941 (1988).
- ⁵(a) Z. Z. Sheng and A. M. Herman, *Nature* **332**, 55 (1988); (b) Z. Z. Sheng, A. M. Herman, A. El Ali, C. Almason, J. Estrada, T. Datta, and R. J. Matson, *Phys. Rev. Lett.* **60**, 937 (1988); (c) Z. Z. Sheng and A. M. Herman, *Nature* **332**, 138 (1988); (d) R. M. Hazen, L. W. Finger, R. J. Angel, C. T. Prewitt, N. L. Ross, C. G. Hadidiacos, P. J. Heaney, D. R. Veblen, Z. Z. Sheng, A. El Ali, and A. M. Herman, *Phys. Rev. Lett.* **60**, 1657 (1988).
- ⁶J. B. Torrance, Y. Tokura, A. Nazzal, and S. S. Parkin, *Phys. Rev. Lett.* **60**, 542 (1988).
- ⁷(a) C. Michel, L. Er-Rakho, and B. Raveau, *Mater. Res. Bull.* **20**, 667 (1985); (b) L. Er-Rakho, C. Michel, and B. Raveau, *J. Solid State Chem.* **73**, 514 (1988).
- ⁸N. Nguyen, J. Choisnet, M. Hervieu, and B. Raveau, *J. Solid State Chem.* **39**, 120 (1981).
- ⁹J. B. Torrance, Y. Tokura, A. I. Nazzal, A. Bezing, T. C. Huang, and S. S. Parkin, *Phys. Rev. Lett.* **61**, 1127 (1988).
- ¹⁰C. Michel and B. Raveau, *Rev. Chem. Miner.* **21**, 407 (1984).
- ¹¹C. Michel and B. Raveau, *J. Solid State Chem.* **43**, 73 (1982); (b) R. M. Hazen *et al.*, *Phys. Rev. B* **35**, 7238 (1987).
- ¹²S. C. Abrahams and J. Kalnajs, *Acta Crystallogr.* **7**, 838 (1954).
- ¹³G. Demazeau, C. Parent, M. Pouchard, and P. Hagenmuller, *Mater. Res. Bull.* **7**, 915 (1972).
- ¹⁴D. W. Margerum, K. L. Chellappa, F. P. Bossu, and G. L. Burce, *J. Amer. Chem. Soc.* **97**, 6894 (1975).
- ¹⁵C. Teske and Hk. Muller-Buschbaum, *Z. Anorg. Allog. Chem.* **371**, 325 (1969).
- ¹⁶(a) Cu^{2+} , Cu^{3+} , O^{2-} , etc., here refer to the formal oxidation states, rather than the actual charge residing on a particular site. In fact, in covalent compounds the actual charge residing on a particular site is considerably reduced than that implied by their formal oxidation states. See, for example, R. T. Sanderson, *Chemical Bonds and Bond Energy* (Academic, New York, 1976); (b) F. P. Basu, K. L. Chellappa, and D. W. Margerum, *J. Amer. Chem. Soc.* **99**, 2195 (1977).
- ¹⁷(a) K. Hestermann and R. Hoppe, *Z. Anorg. Allg. Chem.* **367**, 261 (1969); (b) K. Hestermann and R. Hoppe, *ibid.* **367**, 249 (1969).
- ¹⁸G. Demazeau, B. Buffat, M. Pouchard, and P. Hagenmuller, *J. Solid State Chem.* **54**, 389 (1984).
- ¹⁹L. Vegard, *Z. Phys.* **5**, 17 (1921).
- ²⁰R. D. Shannon and C. T. Prewitt, *Acta Crystallogr. B* **25**, 925 (1969).
- ²¹(a) J. M. Longo and P. M. Racciah, *J. Solid State Chem.* **6**, 526 (1973); (b) B. Grande, Hk. Muller-Buschbaum, and M. Schweizer, *Z. Anorg. Chem.* **428**, 120 (1977).
- ²²C. Teske and Hk. Muller-Buschbaum, *Z. Anorg. Chem.* **379**, 234 (1970).
- ²³B. Grande and Hk. Muller-Buschbaum, *Z. Anorg. Chem.* **417**, 68 (1975).
- ²⁴Hk. Muller-Buschbaum and W. Wollschlager, *Z. Anorg. Allog. Chem.* **414**, 76 (1975).
- ²⁵K. Sreedhar and P. Ganguly (unpublished).
- ²⁶G. Burns, F. H. Dacol, G. Kliche, W. Konig, and M. W. Shafer, *Phys. Rev. B* **37**, 3381 (1988).
- ²⁷F. Gervais, P. Echegut, J. M. Bassat, and P. Odier, *Physica C* **153-155**, 637 (1988).
- ²⁸B. V. Asanov, O. I. Kondratov, N. V. Porotnikov, and K. I. Petrov, *Russ. J. Inorg. Chem.* **33**, 21 (1988).
- ²⁹S. Kemmler-Sack and A. Ehmann, *J. Solid State Chem.* **44**, 366 (1982).
- ³⁰P. Ganguly and N. Y. Vasanthacharya, *J. Solid State Chem.* **61**, 164 (1986).
- ³¹(a) D. Vaknin, S. K. Sinha, D. E. Moncton, D. C. Johnston, J. M. Newsom, C. R. Safinya, and H. E. King, Jr., *Phys. Rev. Lett.* **58**, 2802 (1987); (b) S. Mitsuda, G. Shirane, S. K. Sinha, D. C. Johnston, M. S. Alvarez, D. Vaknin, and D. E. Moncton, *Phys. Rev. B* **36**, 822 (1987); (c) T. Freltoft, J. P. Remeika, D. E. Moncton, A. S. Cooper, J. E. Fischer, D. Harshman, G. Shirane, S. K. Sinha, and D. Vaknin, *ibid.* **B 36**, 826 (1987).
- ³²(a) P. Ganguly and C. N. R. Rao, *Mater. Res. Bull.* **8**, 405 (1973); (b) S. Uchida, H. Takagi, H. Yanagisawa, K. Kishio, K. Kitazawa, K. Fueki, and S. Tanaka, *Jpn. J. Appl. Phys.* **26**, L445 (1987).
- ³³R. L. Greene, H. Maletta, T. S. Plaskett, J. G. Bednorz, and K. A. Muller, *Solid State Commun.* **63**, 379 (1987).
- ³⁴T. Fujita, Y. Aoki, Y. Maeno, J. Sakurai, H. Fukuba, and H. Fujii, *Jpn. J. Appl. Phys.* **26**, L368 (1987).
- ³⁵F. Zuo, X. D. Chen, J. R. Gaines, and A. J. Epstein, *Phys. Rev. B* **38**, 901 (1988).
- ³⁶R. B. van Dover, R. J. Cava, B. Batlogg, and E. A. Rietmann, *Phys. Rev. B* **35**, 5337 (1987).
- ³⁷H. R. Harrison, P. P. Edwards, and J. B. Goodenough, *Philos. Mag.* **B 52**, 679 (1985).
- ³⁸W. E. Farneth, R. S. Mclean, E. M. McCarron III, F. Zuo, Y. Lu, B. R. Patton, and A. J. Epstein, *Phys. Rev. B* **39**, 6594 (1989).
- ³⁹N. F. Mott, *Metal-Insulator Transitions* (Taylor and Francis, London, 1974).
- ⁴⁰(a) N. Nguyen, F. Studer, and B. Raveau, *J. Phys. Chem. Solids* **44**, 389 (1983); (b) J. R. Cooper, B. Alavi, L. W. Zhou, W. P. Beyermann, and G. Gruner, *Phys. Rev. B* **35**, 8794 (1987).
- ⁴¹K. Sreedhar and P. Ganguly, *Inorg. Chem.* **27**, 2261 (1988).
- ⁴²G. A. Sharpataya, Z. P. Ozerova, I. S. Shaplygin, V. B. Lazarev, and A. A. Zakharov, *Russ. J. Inorg. Chem.* **33**, 494 (1988).
- ⁴³P. Ganguly, K. Sreedhar, A. K. Raychaudhuri, and C. N. R. Rao, *Pramana J. Phys.* **27**, 229 (1987).
- ⁴⁴P. Ganguly, N. Y. Vasanthacharya, C. N. R. Rao, and P. P. Edwards, *J. Solid State Chem.* **54**, 400 (1984).
- ⁴⁵P. W. Anderson, *Phys. Rev.* **109**, 1492 (1958).
- ⁴⁶P. W. Anderson, *Science* **235**, 1196 (1987).
- ⁴⁷H. Unoki, Y. Nishihara, K. Oka, M. Tokumoto, and K. Murata, *Physica C* **153-155**, 1481 (1988).
- ⁴⁸N. P. Ong, Z. Z. Wang, J. C. Clayhold, J. M. Tarascon, L. H. Greene, and W. R. Mc Kinnon, *Phys. Rev. B* **35**, 8807 (1987).
- ⁴⁹M. W. Shafer, T. Penney, and B. L. Olson, *Phys. Rev. B* **36**, 4047 (1987).
- ⁵⁰M. Petravic, E. Tutis, A. Hamzic, and L. Forro, *Solid State Commun.* **65**, 573 (1988).

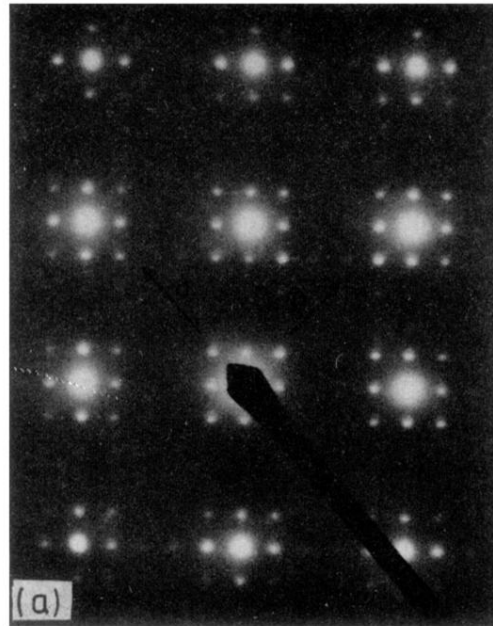


FIG. 4. Typical electron diffraction pattern (a) and lattice image (b) obtained for the $x=1.2$ sample along the [001] direction showing $(5 \times)$ a K_2NiF_4 superlattice and $\sim 18 \text{ \AA}$ fringes.